Published in final edited form as:
Arthritis Rheum. 2008 June ; 58(6): 1674–1686. doi:10.1002/art.23454.

Glucocorticoid Excess in Mice Results in Early Activation of Osteoclastogenesis and Adipogenesis and Prolonged Suppression of Osteogenesis:

A Longitudinal Study of Gene Expression in Bone Tissue From Glucocorticoid-Treated Mice

Wei Yao, MD[1], **Zhiqiang Cheng, MD**[1], **Cheryl Busse, MS**[1], **Aaron Pham, BS**[1], **Mary C. Nakamura, MD**[2], and **Nancy E. Lane, MD**[1]

[1]University of California at Davis Medical Center, Sacramento

[2]University of California, San Francisco

Abstract

Objective—Glucocorticoid (GC) excess induces alterations in bone metabolism that weaken bone structure and increase fracture risk. The aim of this study was to identify genes associated with bone metabolism in GC-treated mice, by performing a microarray analysis.

Methods—Long bones from mice exposed to GC excess were collected after 0, 7, 28, and 56 days of treatment, to measure bone microarchitecture and extract RNA for microarray analyses.

Results—Bone loss in this animal model was confirmed by changes in bone turnover markers as well as bone architecture, as measured by microfocal computed tomography. GC excess induced an early up-regulation of genes involved in osteoclast activation, function, and adipogenesis, which peaked on day 7. The expression of genes associated with osteoclast cytoskeletal reorganization and genes associated with matrix degradation peaked on day 28. On day 28 and day 56, the expression of genes associated with osteoblast activation and maturation was decreased from baseline, while the expression of Wnt antagonists was increased. In addition, the expression of genes expressed in osteocytes associated with bone mineralization was significantly higher at the later time points, day 28 and day 56. Reverse transcription–polymerase chain reaction confirmed the results of microarray analysis in selected genes.

Conclusion—GC excess is associated with early activation of genes associated with osteoclastogenesis and adipogenesis and a later suppression of genes associated with osteogenesis and mineralization. Novel interventions with agents that modulate either Wnt signaling or mineralization may be effective in GC-induced osteoporosis.

Address correspondence and reprint requests to Nancy E. Lane, MD, Department of Internal Medicine, Center for Healthy Aging, 4800 Second Avenue, Suite 2600, University of California at Davis Medical Center, Sacramento, CA 95817. nancy.lane@ucdmc.ucdavis.edu.

AUTHOR CONTRIBUTIONS

Dr. Lane had full access to all of the data in the study and takes responsibility for the integrity of the data and the accuracy of the data analysis.

Study design. Yao, Lane.

Acquisition of data. Yao, Busse, Pham.

Analysis and interpretation of data. Yao, Cheng, Pham, Nakamura, Lane.

Manuscript preparation. Yao, Cheng, Nakamura, Lane.

Statistical analysis. Yao, Lane.

Glucocorticoids (GCs) are frequently prescribed for the treatment of many chronic noninfectious inflammatory disorders, including arthritis, pulmonary diseases, and skin diseases. Although GCs are potent antiinflammatory agents, long-term use results in several adverse side effects, the most common of which is bone loss, which increases the risk of fracture throughout the skeleton (1). Patients treated with GCs have been reported to have an early, rapid increase in bone resorption accompanied by a prolonged reduction in bone formation (2).

The influence of GCs on bone resorption was thought to be indirect and related in part to reduced calcium absorption and increased renal calcium excretion (3). However, recent studies have shown that GCs act directly on osteoclasts to decrease apoptosis of mature osteoclasts (4). Kim et al (5) observed that GCs in vitro inhibited the proliferation of osteoclasts from bone marrow macrophages in a dose-dependent manner. In addition, higher GC doses had no effect on osteoclast maturation but inhibited the ability of osteoclasts to reorganize their cytoskeleton. Therefore, GC excess results in an increased number of osteoclasts but an apparent inhibition of function, with impaired spreading and degrading of mineralized matrix (5).

GCs also alter osteoblast and osteocyte function that contributes to GC-induced osteoporosis (3). GCs directly inhibit cellular proliferation and differentiation of the osteoblast lineage (1), reduce osteoblast maturation and activity (6), and induce osteoblast and osteocyte apoptosis in vivo (7). The suppression of osteoblast function by GCs is reported to be associated with alteration of the Wnt signaling pathway (8), a critical pathway for osteoblastogenesis (9). GCs enhance expression of Dkk-1 (10), one of the Wnt antagonists that prevent soluble Wnt protein from binding to its receptor complex (11). GCs maintain levels of glycogen synthase kinase 3 (GSK3β) (12), a key kinase phosphorylating β-catenin, thereby preventing the translocation of β-catenin into the nucleus and the initiation of transcription in favor of osteoblastogenesis. GCs may also enhance bone marrow stromal cell development toward adipocyte lineage rather than toward osteoblasts (13). Moreover, the loss of osteocytes by GC-induced apoptosis (14) may disrupt the osteocyte–canalicular network, resulting in a failure to direct bone remodeling at the trabecular surface. The GC-induced changes in osteocyte function also result in weakening of the localized material properties around osteocytes as well as whole-bone strength (15).

Information regarding the majority of molecular mechanisms responsible for GC excess was derived from in vitro studies of individual cell lines. Therefore, we hypothesized that expression of osteoblast and osteoclast genes obtained from the long bones of male mice treated with GCs would change over time. To test this hypothesis, we used microarray technology and verified our microarray data by real-time polymerase chain reaction (PCR) analysis of selected genes. In addition, we evaluated the association of gene transcription with changes in bone turnover and whole-bone structural changes in GC-treated mice, and we identified sequential alteration of gene expression in osteoclastogenesis, adipogenesis, and osteogenesis. These data provide in vivo evidence supporting direct or indirect regulation of many new gene transcripts associated with GC excess and enhance our understanding of GC-induced bone loss.

MATERIALS AND METHODS

Animals and experimental procedures

Six-month-old male Swiss Webster mice were obtained from Charles River (San Jose, CA). The mice were maintained on a diet of commercial rodent chow (22/5 Rodent Diet; Harlan Teklad, Madison, WI) with 0.95% calcium and 0.67% phosphate, available ad libitum. The mice were housed in a room that was maintained at a temperature of 70°F, with a 12-hour

light/dark cycle. The mice were randomized by body weight into 5 groups (8–10 mice/group). Slow-release pellets (Innovative Research of America, Sarasota, FL) of placebo or GC (5 mg/kg 60-day slow-release prednisolone pellets) were administered by subcutaneous implantation. Groups of GC-treated mice (n = 7–14 mice/group) were killed on days 0, 7, 28, and 56.

At the time of necropsy, the mice were exsanguinated by cardiac puncture. For all study mice, serum samples were obtained during necropsy and stored at −80°C prior to the assessment of biochemical markers of bone turnover. At the time when the mice were killed, the right femurs were placed in 10% phosphate buffered formalin for 24 hours and then transferred to 70% ethanol for microfocal computed tomography (micro-CT) measurement of 3-dimensional (3-D) bone structure. The fifth lumbar vertebral bodies were embedded in methylmethacrylate and sectioned longitudinally (4-μm–thick sections) with a Leica/Jung 2255 microtome (Leica, Cambridge, UK). Histomorphometric measurement of the adipose tissue area/total tissue area was performed using a Bio-Quant semiautomatic image analysis system (Bio-Quant Image Analysis Corporation, Nashville, TN) linked to a microscope equipped with transmitted and fluorescent light.

Biochemical markers of bone turnover

Serum levels of osteocalcin, type 5b tartrate-resistant acid phosphatase (TRAP5b), and C-telopeptide of type I collagen (CTX) were measured using mouse sandwich enzyme-linked immunosorbent assay kits from Biomedical Technologies (Stroughton, MA), SBA Sciences (Fountain Hills, AZ), or Nordic Bioscience (Chesapeake, VA). The protocols recommended by the manufacturers were followed, and all samples were assayed in duplicate. A standard curve was generated from each kit, and the absolute concentrations were extrapolated from the standard curves. The coefficients of variations for interassay and intraassay measurements were <10% for all assays and are similar to the manufacturers' references (15).

Micro-CT

The right distal femur from each mouse was scanned and measured in vivo using micro-CT (VivaCT 40; Scanco Medical, Bassersdorf, Switzerland), with an isotropic resolution of 10 μm in all 3 spatial dimensions. The scan was initiated at the lateral periosteal margin through the medial periosteal margin of the distal femur, 0.1 mm from the highest part of the growth plate and continuing proximally. Three-dimensional trabecular structure parameters were measured directly, as previously described. Mineralized bone was separated from bone marrow, using a matching cube 3-D segmentation algorithm. Bone volume (BV) was calculated using tetrahedrons corresponding to the enclosed volume of the triangulated surface. Total volume (TV) was the volume of the sample that was examined. A normalized index, BV/TV, was used to compare samples of varying size. The methods used for calculating trabecular thickness, trabecular separation, and trabecular number have been described previously (15).

RNA preparation and hybridization to microarray

Femurs and tibiae, excluding joints and primary metaphyses, were dissected and flash-frozen in liquid nitrogen. Total RNA was isolated using a modified 2-step purification protocol employing homogenization (PRO 250 Homogenizer with a 10-mm × 105-mm generator; PRO Scientific, Oxford, CT) in TRIzol (Invitrogen, Carlsbad, CA), followed by purification over a Qiagen RNeasy column (Qiagen, Valencia, CA).

Purified total RNA (10 μg) from each mouse (3–4 mice per time point) was used for complementary DNA (cDNA) synthesis, which served as a template for in vitro

transcription with biotin incorporation. All microarray analyses were run for individual mice (3–4 mice per group per time point) from GC-treated groups killed on days 0, 7, 28, and 56. Fragmented biotinylated transcripts were hybridized to the Mouse Genome 430 2.0 array (Affymetrix, Santa Clara, CA), according to the manufacturer's protocol. Washing and staining of the arrays were performed on a Fluidics Station 450 (Affymetrix), and the arrays were then scanned using the GeneChip Scanner 3000 (Affymetrix). Raw intensity data for 45,101 probe sets were processed and obtained from the scanned image files, using GeneChip Operating Software (Affymetrix).

Real-time PCR

Real-time PCR was carried out for individual RNA from each animal, on an ABI Prism 7300 (Applied Biosystems, Foster City, CA) in a 25-μl reaction consisting of 12.5 μl 2× SYBR Green Mix (SuperArray, Frederick, MD), 0.2 μl cDNA, 1 μl primer pair mix, and 11.3 μl H_2O. Primer sets for real-time PCR were purchased from SuperArray. Expression of all test genes was relative to expression of a control gene. The results were expressed as fold changes from day 0 (fold change = $2^{-\Delta\Delta C_t}$).

Statistical analysis

The group means and SDs were calculated for all outcome variables. Repeated-measures analysis of variance (ANOVA) (SPSS version 10 software; SPSS, Chicago, IL) was used to assess the differences in bone turnover markers and bone microarchitecture parameters between the GC-treated and placebo groups on days 0, 28, and 56. For all analyses, *P* values less than 0.05 were considered significant.

For microarray analysis, the array files were exported to ArrayAssist version 3.2 (Affymetrix) for model-based expression, normalization, and probe summarization using the GC–robust multichip analysis (RMA) algorithm. GC-RMA data were $\log_2$-transformed and centered relative to the control group (day 0). The filtered probe sets served as the working set for further statistical analysis using unpaired *t*-tests with unequal variances. Probabilities were adjusted by the false-discovery rate of <1%, using ANOVA with unequal variances and the Benjamini and Hochberg correlation for multiple comparisons between time points. By using this approach, no more than 1% of the false-positive genes were in the list of significantly changed genes at each time point.

Finally, we further filtered the genes with >2-fold changes, to achieve more strict selection of significantly changed genes. The results of the significance analyses passing the significance level were further analyzed using GeneShifter software (GeneShifter, Seattle, WA), grouped by gene functions. The pathway information in GeneShifter is derived from the Kyoto Encyclopedia of Genes and Genomes pathway annotations via genes in Entrez (National Center for Biotechnology Information, Bethesda, MD). If a gene is listed in a pathway, it does not necessarily mean that the gene is part of that biologic pathway. The gene could be involved upstream or could be the result of pathway activation. Different software packages differ in terms of the manner in which genes are listed within pathways.

RESULTS

Effect of GCs on trabecular bone mass, bone resorption, and bone formation

In order to determine the in vivo efficacy of our GC-induced osteoporosis model, we performed biochemical analysis of bone turnover markers and micro-CT to evaluate trabecular bone microarchitecture. Serum osteoclast activity, as assessed by measuring levels of CTX, was increased by nearly 80% between day 7 and day 28 and remained 26% above baseline levels on day 56. The level of osteocalcin, a marker of osteoblast function,

started to decrease on day 7 and was decreased by 50% from day 28 to day 56. By day 28, trabecular bone volume at the distal femur had decreased by 16% compared with baseline levels in GC-treated mice, and this decrease remained unchanged on day 56 (Figure 1). These data, together with results of previous studies using similar mouse models of GC excess (7,15), suggest that GC excess in a small in vivo animal model increases bone resorption during the early phase of GC excess and decreases bone formation with prolonged exposure, such that there is a rapid decline in trabecular bone volume and the volume remains low.

Effect of GC excess in vivo on gene expression critical for osteoclast activation and function

After we established that GC excess in vivo increased bone resorption, a time course for the gene expression of factors critical for osteoclast activation and differentiation was determined. The expression of *Csf1* and its receptor, *c-fms*, which promote osteoclast proliferation, differentiation, and survival (16), was up-regulated by ~2-fold in GC-treated mice on day 7 compared with day 0 (Table 1). Genes associated with integrin-mediated signaling, including *Ibsp*, *Itgb3* (17), disintegrin, and *Adam8* (18), were generally up-regulated on day 7 (*Ibsp*) or day 28 through day 56 (*Itgb3* and *Adam8*) (Table 1 and Figure 2).

Genes associated with pathways that were significantly up-regulated within integrin signaling were those associated with the actin cytoskeleton, focal adhesion, leukocyte transendothelial migration, and extracellular matrix receptor interaction pathways (Figure 2). All of these pathways are critical for the attachment of osteoclasts to the bone surface and for preparing osteoclasts to resorb bone matrix. Genes associated with activation of the immunoreceptor tyrosine–based activation motif (ITAM) pathway, which include Fcγ receptor (19), an osteoclast-associated receptor (*Oscar*), a triggering receptor expressed on myeloid cells (*Trem2*), and a receptor for DNAX activation protein 12 (*Dap12*) (20), were up-regulated from day 7 to day 56 (Table 1). Interestingly, gene expression of RANKL (21) and RANK, a key receptor for this osteoclast-activating cytokine, was not significantly different from that on day 0, as measured either by microarray on days 7, 28, and 56 or by reverse transcription (RT)–PCR on days 1, 3, 7, 28, and 56 (data not shown). Transcripts for signaling molecules and the critical transcription factors reported to be associated with osteoclast differentiation (*PLC*γ and *Nfatc1*) (22) were up-regulated on days 7 and 28 (Table 1). Transcripts that are associated with changes in osteoclast cytoskeleton organization (*c-Src*, *Syk*, and *Vav3*) (23) were also up-regulated on days 7, 28, and 56 (Table 1).

Genes that are essential for bone matrix degradation as well as regulation of the complement and coagulation cascades pathway (Figure 3), such as ATPase, cathepsins S, H, K, G, and C, matrix metalloproteinases 8, 9, 13, and 19, and serine proteases 15 and 22, were significantly up-regulated on days 28 and 56 (Table 1 and Figure 3) compared with day 0. Although changes in some of these genes, such as *Ctsk*, *Trem2*, *Dap12*, and *Oscar*, are likely attributable to specific changes in osteoclasts, many of the changes could also be attributable to changes in gene transcription in other cell types present in the bone marrow microenvironment.

Effect of GC excess on gene expression that supports adipocyte differentiation

The expression of transcription factors for adipocyte early differentiation (CCAAT/enhancer binding protein α [c/EBPα], c/EBPβ, peroxisome proliferator–activated receptor γ [PPARγ], and PPARσ) was increased on day 7 but did not differ from day 0 levels thereafter (Table 2). In contrast, the expression of *AdipoQ*, a marker for mature adipocytes, remained increased throughout the study period. A quantitative assessment of the percentage of adipose tissue in

the secondary spongiosa of the fifth lumbar vertebral body showed that the adipose tissue area/total tissue area was increased by 18% in the GC-treated group compared with the placebo group on day 56 (mean ± SD 7.62 ± 0.6% versus 6.48 ± 0.8%; $P < 0.05$).

Effect of GC excess in vivo on suppression of gene expression critical for osteoblast differentiation and maturation

Growth factors that affect osteoblastogenesis (transforming growth factor β1 [TGFβ1] and bone morphogenetic protein 2 [BMP-2]) (24) were down-regulated on day 28 and day 56. Wnt signaling inhibitors, such as Dkk-1, Wnt inhibitory factor 1 (WNF-1), and sclerostin (11), which are reported to antagonize Wnt stimulation of osteoblast differentiation, were up-regulated on day 56 (Figures 4–6). Receptors for Wnt proteins, including Frizzled proteins 4 and 7, which regulate osteoblast differentiation (25), and Wnt transcriptional gene *LEF1* (Figure 5) were down-regulated on day 7. The alkaline phosphatase gene (*Akp2*), which reflects osteoblast differentiation, was suppressed from day 7 to day 56 (Figure 6). The expression of integrins that are expressed by osteoblasts and are associated with osteoblast maturation, such as integrin subunits α5, α7, β4, β5, and β6 (26), was down-regulated on days 28 and 56 (Figure 2). Moreover, the expression of genes expressed primarily by osteocytes associated with bone mineralization (*Dmp1* and *Phex*) (27) was increased on day 28, and β4, β5, and β6 remained at day 56 (Figures 5 and 6). Thus, GC excess in vivo induced suppression of transcription of genes for osteoblast differentiation involved in the regulation of the MAPK, TGFβ1, hedgehog, and Wnt signaling pathways (Figure 5).

DISCUSSION

Mice with long-term exposure to GCs had altered bone metabolism that resulted in a rapid loss of trabecular bone for the first 28 days, followed by a slower loss of trabecular bone thereafter. Also, GC excess significantly changed osteocytic gene expression (*Dmp1*, *Phex*, and *Sost*), which may be associated with osteocyte viability and function, as has been previously reported (15).

Osteoclasts are known to be activated by several pathways, including RANKL/RANK, macrophage colony-stimulating factor/*c-fms*, tumor necrosis factor α [TNFα]/TNF receptor, and ITAM, that signal through phospholipase Cγ and phosphatidylinositol 3-kinase, which ultimately activate the critical transcription factor, nuclear factor of activated T cells c1, to stimulate osteoclast differentiation and activity (28). Our current in vivo study provides evidence that GCs activate osteoclastogenesis in a time-dependent manner, with early increased expression of genes associated with osteoclast activation, maturation, and function. This time course correlates with the GC-induced bone loss observed in clinical studies (6,15). Interestingly, osteoprotegerin gene expression was reported to be reduced when isolated human primary osteoblasts or dendritic cells were treated with GCs (29,30). In contrast, we did not detect changes in gene expression for osteoprotegerin, RANK, or RANKL by either microarray or RT-PCR performed with whole-bone RNA on days 1, 3, 7, 28, and 56 (data not shown). The differences in these studies could be attributable to either the effects of multiple cellular interactions in vivo compared with direct effects observed in vitro or differential dose effects. Additional studies that evaluate a dose response will be needed to further investigate the changes in RANK/RANKL expression during GC-induced bone loss in vivo. This rapid increase in the expression of genes involved with osteoclast maturation and function was associated with an increase in osteoclast surface and bone resorption. This, over time, can lead to a rapid reduction in bone mass and bone strength over a very short period of time.

In vivo GC excess increased the number of osteoclasts on the trabecular bone surface after 1 week of GC exposure, and this was associated with up-regulated transcripts of signaling intermediates (*Syk*, *c-Src*, *Vav3*) that are reported to play a role in osteoclast cytoskeletal rearrangement. Cytoskeletal proteins most likely enable the osteoclast to spread across the trabecular surface, forming actin rings and ruffled membranes that are essential for matrix degradation (23,31). Interestingly, Kim et al reported that osteoclasts exposed to high-dose dexamethasone failed to spread and resorb bone in vitro (5). When we exposed mice to low-dose GCs for 56 days to mimic the physiologic changes following GC administration in clinical practice (32), transcriptional changes from the microarray analysis were compared with bone histomorphometry, and we observed increased osteoclast surface and osteoclast numbers on the trabecular bone surface (15,33). Furthermore, biochemical markers of bone turnover, including TRAP5b (data not shown) and CTX, were also increased in association with GC excess. The increased osteoclast activity may partially account for the reduction in trabecular bone volume observed with GC excess.

Osteogenesis and adipogenesis are thought to share common bone marrow stromal progenitors (34). Under different culture conditions, osteogenic cells and adipocytes can change their cell phenotype (35,36). Growth hormone can influence the lineage choice of osteogenesis or adipogenesis from mesenchymal stem cells (37). Mice that were deficient in thyroid hormone receptors had increased adipogenesis and decreased bone mineral density (38). GC excess provides a potent stimulus for adipogenesis in patients with Cushing's syndrome (39). In cell lines and human preadipocyte cultures, GCs can rapidly stimulate preadipocyte differentiation into adipocytes and also prolong the life span of preadipocytes (40). We observed that the expression of transcription factors for early adipocyte differentiation (c/EBPα, c/EBPβ, and PPARγ) increased rapidly on day 7 and returned to day 0 levels thereafter. However, the level of *AdipoQ*, a gene marker for the differentiated adipocytes, remained elevated throughout the study. Also, the percentage of adipose tissue area in the lumbar vertebral bodies was increased by 18% in the GC-treated mice on day 56 compared with the baseline level. It is possible that GCs may preferentially stimulate the differentiation of stromal cells and preadipocytes to adipocytes, thereby reducing the pool of progenitor cells to differentiate into osteoblasts. This potential mechanism requires further investigation.

The mechanisms that account for GC-induced inhibition of bone formation are not clear. However, a reduced life span and reduced activity of osteoblasts have been described (6). We observed that many transcripts associated with osteoblast maturation and function did not change significantly until after 28 days of GC treatment, and that growth factors such as BMP-2 and TGFβ1 that stimulate osteoblast proliferation were down-regulated from day 28 to day 56.

Wnt signaling regulates many aspects of osteoblast differentiation, function, and death (41). The binding of Wnt proteins to the Frizzled receptor stabilizes β-catenin in the cytoplasm, which would otherwise be phosphorylated with a complex consisting of GSK3β, Axin, Frat-1, and Disheveled proteins. If β-catenin accumulates and is translocated to the nucleus, it binds to transcription factor/lymphoid enhancer binding factor, causing displacement of transcriptional corepressors and inducing gene expression favoring bone formation (42). Wnt signaling can be blocked by interactions with inhibitory factors including WNF-1, secreted Frizzled receptor protein, or the Dkk-1/Kremen complex (43). One other Wnt antagonist is sclerostin, a soluble factor that is secreted mainly by osteocytes (44), binds to low-density lipoprotein receptor–related protein 5/6, and antagonizes canonical Wnt signaling (25). Increased sclerostin expression in osteocytes has been reported to reduce bone formation by promoting osteoblast apoptosis (45).

GCs increase the expression of Dkk-1 in primary human osteoblasts (10). In osteoblastic cell lines, GC excess increases the gene expression of Wnt inhibitors such as Dkk-1, Frizzled 2, Frizzled 7, and Wnt-induced signaling protein 1, and this may partially explain GC-induced suppression of osteoblast function (46). In vivo, GC excess up-regulated the Wnt antagonists (Dkk-1, WNF-1, and Sost) and down-regulated the Wnt receptor complex (Frizzled 4, Frizzled 7, *Dsh1*, and *Axin1*). Importantly, suppression of Wnt signaling was associated with suppressed osteoblast differentiation (*Akp2*) and maturation (osteocalcin) and decreased osteoblastic surface and activity (15).

GCs may also directly affect osteocytes, because the genes primarily expressed in osteocytes, *Dmp1* and *Phex* (47), were up-regulated on days 28 and 56 of GC treatment as compared with day 0. Osteocytes connect to the bone surface via a canalicular system and secrete proteins (dentin matrix protein 1 [DMP1] and PHEX) that modify periosteocytic mineralization (48). For example, DMP1, in its native form, is an acidic phosphorylated extracellular matrix protein that may acidify the perilacunae space and prevent mineralization (49). When *Dmp1* is dephosphorylated, it can then serve as hydroxylapatite nucleator and initiate mineralization (49). Immunohistochemical staining of phosphorylated *Dmp1* was greatly increased in the area surrounding the osteocytes and in the remodeling units (data not shown), corresponding to the low-mineralization regions we previously reported to be associated with GC excess (15). Our microarray analysis provides evidence that GC excess alters osteocyte gene expression. Changes in osteocyte gene expression likely contribute to the localized changes in the bone mineral and elastic modulus around the osteocytes observed in GC-treated patients, which may explain the increased bone fragility that is independent of the bone mass (50). Interventions that target osteocytes may be a possible approach for the prevention and treatment of GC-induced osteoporosis, but additional experiments will need to be performed to study the efficacy of this method.

A limitation of this study is the performance of microarray analysis using whole bone and bone marrow RNA samples; we could not distinguish whether the GC-induced transcriptional changes reflected changes in cellular composition or the response of a particular cell type. In addition, due to limitations with respect to the microarray software, we had to include some transcripts in the heat map that were not significantly related to our research interests or were not significantly related to the pathways studied.

In summary, GC excess is associated with early activation of genes associated with osteoclastogenesis and adipogenesis and a later suppression of genes associated with osteogenesis and mineralization. These changes in gene expression may correspond to the alterations in bone metabolism with GC exposure that result in rapid bone loss. Novel interventions with agents that modulate either Wnt signaling or mineralization may be effective in GC-induced osteoporosis.

Acknowledgments

Supported by the NIH (grants R01-AR-043052-07, 1-K24-AR-48841-02, and 1-K12-HD-05195801, co-funded by the National Institute of Child Health and Human Development, the Office of Research on Women's Health, the Office of Dietary Supplements, and the National Institute on Aging). Dr. Lane holds the Endowed Chair in Aging at the University of California at Davis Medical School.

References

1. Canalis E, Bilezikian JP, Angeli A, Giustina A. Perspectives on glucocorticoid-induced osteoporosis [review]. Bone. 2004; 34:593–8. [PubMed: 15050888]
2. Dempster DW. Bone histomorphometry in glucocorticoid-induced osteoporosis [review]. J Bone Miner Res. 1989; 4:137–41. [PubMed: 2658477]

3. Mazziotti G, Angeli A, Bilezikian JP, Canalis E, Giustina A. Glucocorticoid-induced osteoporosis: an update [review]. Trends Endocrinol Metab. 2006; 17:144–9. [PubMed: 16678739]
4. Jia D, O'Brien CA, Stewart SA, Manolagas SC, Weinstein RS. Glucocorticoids act directly on osteoclasts to increase their life span and reduce bone density. Endocrinology. 2006; 147:5592–9. [PubMed: 16935844]
5. Kim HJ, Zhao H, Kitaura H, Bhattacharyya S, Brewer JA, Muglia LJ, et al. Glucocorticoids suppress bone formation via the osteoclast. J Clin Invest. 2006; 116:2152–60. [PubMed: 16878176]
6. Weinstein RS. Glucocorticoid-induced osteoporosis [review]. Rev Endocr Metab Disord. 2001; 2:65–73. [PubMed: 11708295]
7. Weinstein RS, Jilka RL, Parfitt AM, Manolagas SC. Inhibition of osteoblastogenesis and promotion of apoptosis of osteoblasts and osteocytes by glucocorticoids: potential mechanisms of their deleterious effects on bone. J Clin Invest. 1998; 102:274–82. [PubMed: 9664068]
8. Ohnaka K, Tanabe M, Kawate H, Nawata H, Takayanagi R. Glucocorticoid suppresses the canonical Wnt signal in cultured human osteoblasts. Biochem Biophys Res Commun. 2005; 329:177–81. [PubMed: 15721290]
9. Krishnan V, Bryant HU, MacDougald OA. Regulation of bone mass by Wnt signaling [review]. J Clin Invest. 2006; 116:1202–9. [PubMed: 16670761]
10. Ohnaka K, Taniguchi H, Kawate H, Nawata H, Takayanagi R. Glucocorticoid enhances the expression of dickkopf-1 in human osteoblasts: novel mechanism of glucocorticoid-induced osteoporosis. Biochem Biophys Res Commun. 2004; 318:259–64. [PubMed: 15110782]
11. Li J, Sarosi I, Cattley RC, Pretorius J, Asuncion F, Grisanti M, et al. Dkk1-mediated inhibition of Wnt signaling in bone results in osteopenia. Bone. 2006; 39:754–66. [PubMed: 16730481]
12. Smith E, Frenkel B. Glucocorticoids inhibit the transcriptional activity of LEF/TCF in differentiating osteoblasts in a glycogen synthase kinase-3β-dependent and -independent manner. J Biol Chem. 2005; 280:2388–94. [PubMed: 15537647]
13. Ito S, Suzuki N, Kato S, Takahashi T, Takagi M. Glucocorticoids induce the differentiation of a mesenchymal progenitor cell line, ROB-C26 into adipocytes and osteoblasts, but fail to induce terminal osteoblast differentiation. Bone. 2007; 40:84–92. [PubMed: 16949358]
14. O'Brien CA, Jia D, Plotkin LI, Bellido T, Powers CC, Stewart SA, et al. Glucocorticoids act directly on osteoblasts and osteocytes to induce their apoptosis and reduce bone formation and strength. Endocrinology. 2004; 145:1835–41. [PubMed: 14691012]
15. Lane NE, Yao W, Balooch M, Nalla RK, Balooch G, Habelitz S, et al. Glucocorticoid-treated mice have localized changes in trabecular bone material properties and osteocyte lacunar size that are not observed in placebo-treated or estrogen-deficient mice. J Bone Miner Res. 2006; 21:466–76. [PubMed: 16491295]
16. Faccio R, Takeshita S, Zallone A, Ross FP, Teitelbaum SL. c-Fms and the $\alpha v\beta 3$ integrin collaborate during osteoclast differentiation. J Clin Invest. 2003; 111:749–58. [PubMed: 12618529]
17. Teitelbaum SL. Osteoclasts and integrins. Ann N Y Acad Sci. 2006; 1068:95–9. [PubMed: 16831909]
18. Choi SJ, Han JH, Roodman GD. ADAM8: a novel osteoclast stimulating factor. J Bone Miner Res. 2001; 16:814–22. [PubMed: 11341326]
19. Kim K, Kim JH, Lee J, Jin HM, Lee SH, Fisher DE, et al. Nuclear factor of activated T cells c1 induces osteoclast-associated receptor gene expression during tumor necrosis factor-related activation-induced cytokine-mediated osteoclastogenesis. J Biol Chem. 2005; 280:35209–16. [PubMed: 16109714]
20. Humphrey MB, Ogasawara K, Yao W, Spusta SC, Daws MR, Lane NE, et al. The signaling adapter protein DAP12 regulates multinucleation during osteoclast development. J Bone Miner Res. 2004; 19:224–34. [PubMed: 14969392]
21. Lacey DL, Timms E, Tan HL, Kelley MJ, Dunstan CR, Burgess T, et al. Osteoprotegerin ligand is a cytokine that regulates osteoclast differentiation and activation. Cell. 1998; 93:165–76. [PubMed: 9568710]
22. Takayanagi H, Kim S, Taniguchi T. Signaling crosstalk between RANKL and interferons in osteoclast differentiation. Arthritis Res. 2002; 4 (Suppl 3):S227–32. [PubMed: 12110142]

23. Zou W, Kitaura H, Reeve J, Long F, Tybulewicz VL, Shattil SJ, et al. Syk, c-Src, the $\alpha_v\beta_3$ integrin, and ITAM immunoreceptors, in concert, regulate osteoclastic bone resorption. J Cell Biol. 2007; 176:877–88. [PubMed: 17353363]
24. Rawadi G, Vayssiere B, Dunn F, Baron R, Roman-Roman S. BMP-2 controls alkaline phosphatase expression and osteoblast mineralization by a Wnt autocrine loop. J Bone Miner Res. 2003; 18:1842–53. [PubMed: 14584895]
25. Vaes BL, Dechering KJ, van Someren EP, Hendriks JM, van de Ven CJ, Feijen A, et al. Microarray analysis reveals expression regulation of Wnt antagonists in differentiating osteoblasts. Bone. 2005; 36:803–11. [PubMed: 15820155]
26. Roman-Roman S, Garcia T, Jackson A, Theilhaber J, Rawadi G, Connolly T, et al. Identification of genes regulated during osteoblastic differentiation by genome-wide expression analysis of mouse calvaria primary osteoblasts in vitro. Bone. 2003; 32:474–82. [PubMed: 12753863]
27. Feng JQ, Ward LM, Liu S, Lu Y, Xie Y, Yuan B, et al. Loss of DMP1 causes rickets and osteomalacia and identifies a role for osteocytes in mineral metabolism. Nat Genet. 2006; 38:1310–5. [PubMed: 17033621]
28. Baron R. Arming the osteoclast. Nat Med. 2004; 10:458–60. [PubMed: 15122243]
29. Hofbauer LC, Khosla S, Dunstan CR, Lacey DL, Boyle WJ, Riggs BL. The roles of osteoprotegerin and osteoprotegerin ligand in the paracrine regulation of bone resorption [review]. J Bone Miner Res. 2000; 15:2–12. [PubMed: 10646108]
30. Schoppet M, Henser S, Ruppert V, Stubig T, Al-Fakhri N, Maisch B, et al. Osteoprotegerin expression in dendritic cells increases with maturation and is NF-κB-dependent. J Cell Biochem. 2007; 100:1430–9. [PubMed: 17171649]
31. Faccio R, Teitelbaum SL, Fujikawa K, Chappel J, Zallone A, Tybulewicz VL, et al. Vav3 regulates osteoclast function and bone mass. Nat Med. 2005; 11:284–90. [PubMed: 15711558]
32. Saag KG. Glucocorticoid-induced osteoporosis [review]. Endocrinol Metab Clin North Am. 2003; 32:135–57. vii. [PubMed: 12699296]
33. Weinstein RS, Jia D, Powers CC, Stewart SA, Jilka RL, Parfitt AM, et al. The skeletal effects of glucocorticoid excess override those of orchidectomy in mice. Endocrinology. 2004; 145:1980–7. [PubMed: 14715712]
34. Blair HC, Sun L, Kohanski RA. Balanced regulation of proliferation, growth, differentiation, and degradation in skeletal cells. Ann N Y Acad Sci. 2007; 1116:165–73. [PubMed: 17646258]
35. Bennett JH, Joyner CJ, Triffitt JT, Owen ME. Adipocytic cells cultured from marrow have osteogenic potential. J Cell Sci. 1991; 99 (Pt 1):131–9. [PubMed: 1757497]
36. Schiller PC, D'Ippolito G, Brambilla R, Roos BA, Howard GA. Inhibition of gap-junctional communication induces the trans-differentiation of osteoblasts to an adipocytic phenotype in vitro. J Biol Chem. 2001; 276:14133–8. [PubMed: 11278824]
37. Gevers EF, Loveridge N, Robinson IC. Bone marrow adipocytes: a neglected target tissue for growth hormone. Endocrinology. 2002; 143:4065–73. [PubMed: 12239118]
38. Kindblom JM, Gevers EF, Skrtic SM, Lindberg MK, Gothe S, Tornell J, et al. Increased adipogenesis in bone marrow but decreased bone mineral density in mice devoid of thyroid hormone receptors. Bone. 2005; 36:607–16. [PubMed: 15780976]
39. Boscaro M, Barzon L, Fallo F, Sonino N. Cushing's syndrome [review]. Lancet. 2001; 357:783–91. [PubMed: 11253984]
40. Tomlinson JJ, Boudreau A, Wu D, Atlas E, Hache RJ. Modulation of early human preadipocyte differentiation by glucocorticoids. Endocrinology. 2006; 147:5284–93. [PubMed: 16873539]
41. Johnson ML, Harnish K, Nusse R, Van Hul W. LRP5 and Wnt signaling: a union made for bone. J Bone Miner Res. 2004; 19:1749–57. [PubMed: 15476573]
42. Nusse R. The Wnt gene family in tumorigenesis and in normal development. J Steroid Biochem Mol Biol. 1992; 43:9–12. [PubMed: 1388050]
43. Byun T, Karimi M, Marsh JL, Milovanovic T, Lin F, Holcombe RF. Expression of secreted Wnt antagonists in gastrointestinal tissues: potential role in stem cell homeostasis. J Clin Pathol. 2005; 58:515–9. [PubMed: 15858124]

44. Winkler DG, Sutherland MK, Geoghegan JC, Yu C, Hayes T, Skonier JE, et al. Osteocyte control of bone formation via sclerostin, a novel BMP antagonist. EMBO J. 2003; 22:6267–76. [PubMed: 14633986]
45. Poole KE, van Bezooijen RL, Loveridge N, Hamersma H, Papapoulos SE, Lowik CW, et al. Sclerostin is a delayed secreted product of osteocytes that inhibits bone formation. FASEB J. 2005; 19:1842–4. [PubMed: 16123173]
46. Hurson CJ, Butler JS, Keating DT, Murray DW, Sadlier DM, O'Byrne JM, et al. Gene expression analysis in human osteoblasts exposed to dexamethasone identifies altered developmental pathways as putative drivers of osteoporosis. BMC Musculoskelet Disord. 2007; 8:12. [PubMed: 17295923]
47. Rios HF, Ye L, Dusevich V, Eick D, Bonewald LF, Feng JQ. DMP1 is essential for osteocyte formation and function. J Musculoskelet Neuronal Interact. 2005; 5:325–7. [PubMed: 16340123]
48. Narayanan K, Ramachandran A, Hao J, He G, Park KW, Cho M, et al. Dual functional roles of dentin matrix protein 1: implications in biomineralization and gene transcription by activation of intracellular Ca^{2+} store. J Biol Chem. 2003; 278:17500–8. [PubMed: 12615915]
49. Tartaix PH, Doulaverakis M, George A, Fisher LW, Butler WT, Qin C, et al. In vitro effects of dentin matrix protein-1 on hydroxyapatite formation provide insights into in vivo functions. J Biol Chem. 2004; 279:18115–20. [PubMed: 14769788]
50. Van Staa TP, Laan RF, Barton IP, Cohen S, Reid DM, Cooper C. Bone density threshold and other predictors of vertebral fracture in patients receiving oral glucocorticoid therapy. Arthritis Rheum. 2003; 48:3224–9. [PubMed: 14613287]

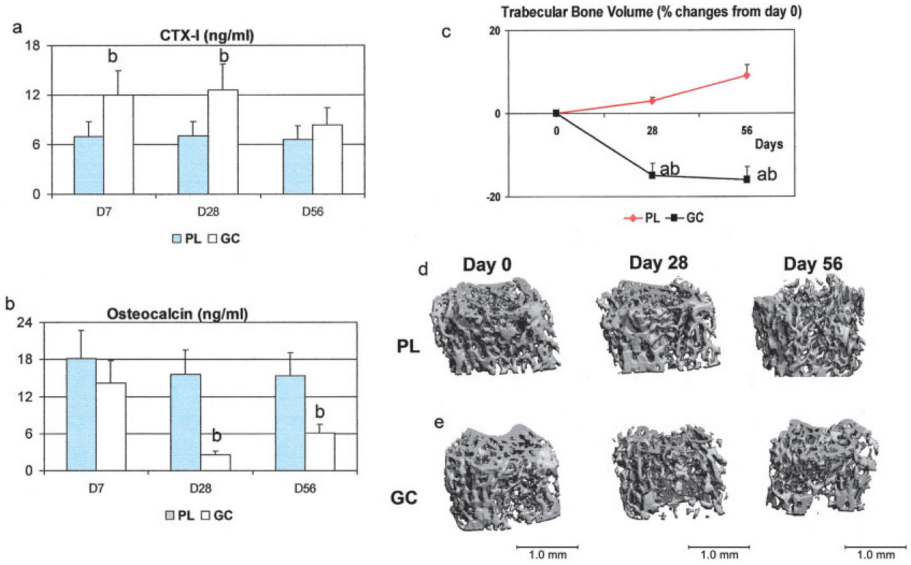

Figure 1.

Time-dependent changes in bone turnover markers and bone microarchitecture associated with glucocorticoid (GC) excess. **a,** Levels of C-telopeptide of type I collagen (CTX), a marker for osteoclast resorption, showing an increase of ~40% on days 7 and 28 in GC-treated mice compared with placebo (PL)–treated mice. **b,** Levels of osteocalcin, showing a decrease of ~50% on days 28 and 56 in GC-treated mice compared with placebo-treated mice. **c–e,** Trabecular bone volume, as measured by repeated in vivo microfocal computed tomography at the distal femurs. The volume decreased by nearly 20% from day 0 to day 28 and then leveled off. Values in **a–c** are the mean and SD. a = $P < 0.05$ versus day 0; b = $P < 0.05$ versus placebo at the same time point.

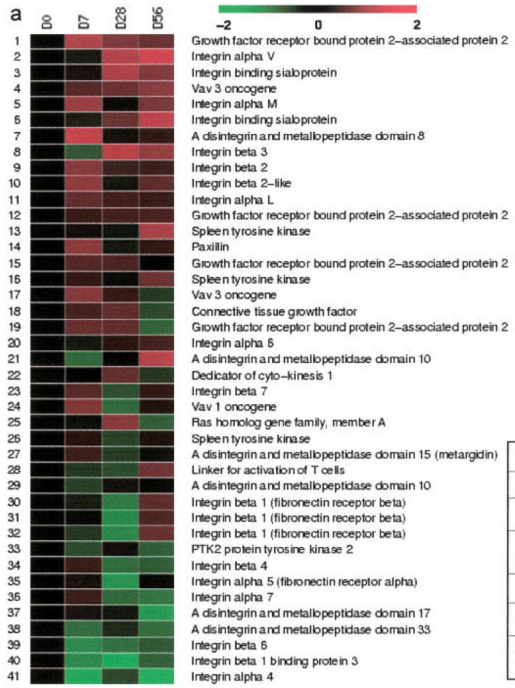

b

KEGG Pathway	Z Score
Regulation of actin cytoskeleton	10.61
Focal adhesion	8.59
Leukocyte transendothelial migration	8.30
ECM-receptor interaction	8.21
Cell adhesion molecules (CAMs)	5.03
Natural killer cell mediated cytotoxicity	5.36

Figure 2.

Time-dependent gene profiling of integrin-mediated signaling associated with glucocorticoid excess. **a,** Heat map of the integrin-mediated pathway. Red indicates up-regulation, and green indicates down-regulation compared with day 0. Up-regulated genes included αv integrin, αM integrin, β3 integrin, and Vav3; up-regulation was at its highest level on day 28. Down-regulated genes included β1 integrin, β4 integrin, α5 integrin, β6 integrin, β7 integrin, ADAM-17, and ADAM-33. **b,** Main biologic Kyoto Encyclopedia of Genes and Genomes (KEGG) pathways of integrin-mediated signaling. ECM = extracellular matrix.

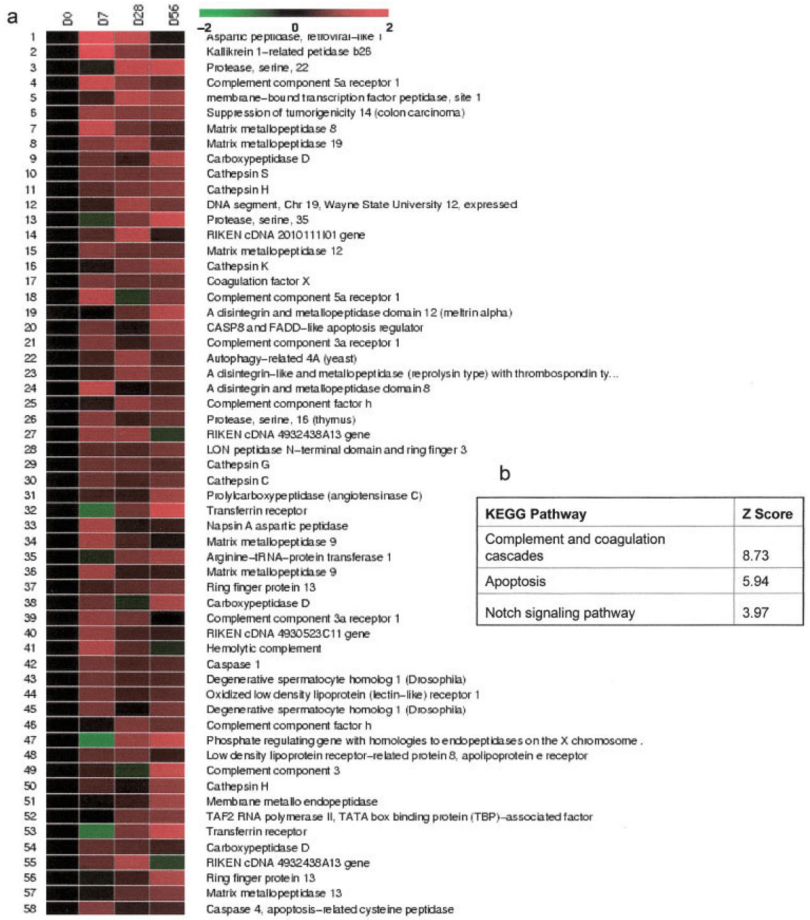

b

KEGG Pathway	Z Score
Complement and coagulation cascades	8.73
Apoptosis	5.94
Notch signaling pathway	3.97

Figure 3.

Time-dependent gene profiling of matrix proteolysis associated with glucocorticoid excess. **a,** Heat map of the matrix proteolysis pathway. Red indicates up-regulation, and green indicates down-regulation compared with day 0. Up-regulated genes included serine proteases 22 and 35, matrix metalloproteinase 8 (MMP-8), MMP-9, MMP-12, MMP-19, and cathepsins S, H, K, G, and C. **b,** Main biologic Kyoto Encyclopedia of Genes and Genomes (KEGG) pathways of matrix proteolysis.

KEGG Pathway	Z Score
Wnt signaling pathway	21.16
Adherens junction	9.05
Tight junction	4.76
Hedgehog signaling pathway	5.92
Gap junction	4.18

Figure 4.

Time-dependent gene profiling of Wnt receptor signaling associated with glucocorticoid excess. **a,** Heat map of the Wnt receptor signaling pathway. Red indicates up-regulation, and green indicates down-regulation compared with day 0. Up-regulated genes included Wnt inhibitors such as Dkk-1 and Wnt inhibitory factor 1. Down-regulated genes included *Lrp1*, *Dsh1*, *Axin1*, and Frizzled 7; down-regulation was most significant on either day 28 or day 56. **b,** Main biologic Kyoto Encyclopedia of Genes and Genomes (KEGG) pathways of Wnt receptor signaling.

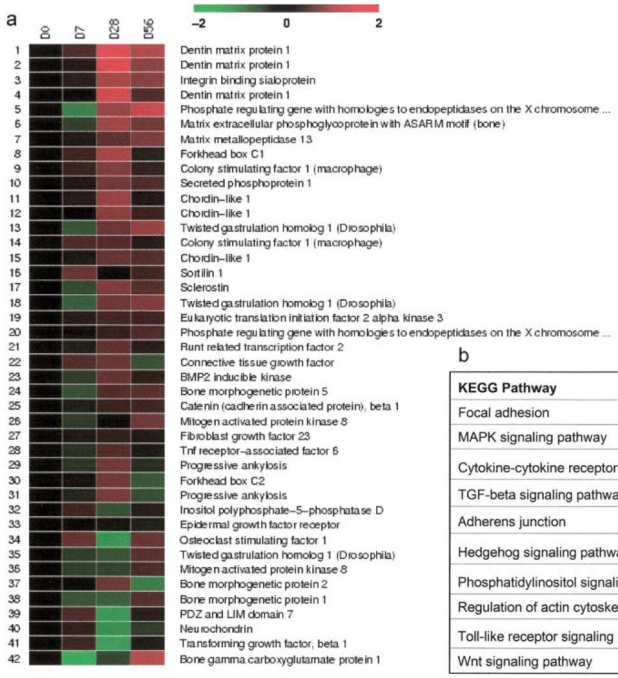

b

KEGG Pathway	Z Score
Focal adhesion	5.54
MAPK signaling pathway	4.32
Cytokine-cytokine receptor interaction	3.74
TGF-beta signaling pathway	5.72
Adherens junction	5.12
Hedgehog signaling pathway	4.18
Phosphatidylinositol signaling system	4.32
Regulation of actin cytoskeleton	1.62
Toll-like receptor signaling pathway	3.13
Wnt signaling pathway	2.12

Figure 5.

Time-dependent gene profiling of bone remodeling associated with glucocorticoid excess. **a,** Heat map of the bone remodeling pathway. Red indicates up-regulation, and green indicates down-regulation compared with day 0. Up-regulated genes included *Dmp1*, *Phex*, *Csf1*, and *Sost*; up-regulation was most significant on days 28 and 56. Down-regulated genes included *Bmp2* and *TGFB1*; down-regulation was most significant on day 28 for *TGFB1* and day 56 for *Bmp2*. **b,** Kyoto Encyclopedia of Genes and Genomes (KEGG) pathways of bone remodeling overlapped with the above biologic pathways, as in Figures 2–4. TGF = transforming growth factor.

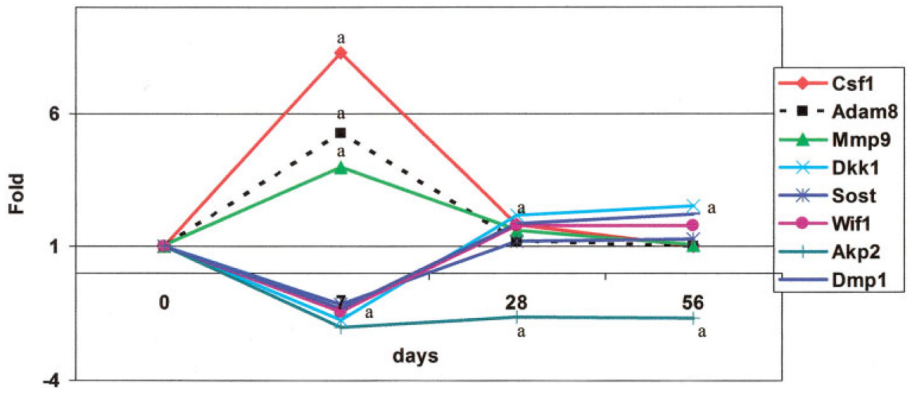

Figure 6.

Time course of changes in the expression of selected genes involved in osteoclastogenesis, in association with glucocorticoid excess, as determined by polymerase chain reaction. The expression of *Csf1*, *Adam8*, and *Mmp9*, which was significantly up-regulated on day 7, remained ~2-fold higher than the day 0 level until day 56. The expression of Wnt inhibitors, including Dkk-1, *Sost*, and *WNF1*, was increased from day 28 to day 56. Expression of the gene that represented osteoblast differentiation, *Akp2*, was suppressed throughout the study. The level of *Dmp1*, which is expressed by osteoblasts and osteocytes, was increased on days 28 and 56. a = $P < 0.05$ versus day 0.

Table 1

Time-dependent effects of glucocorticoid excess on osteoclastogenesis*

Gene symbol	Gene name	Gene function	Day 7	Day 28	Day 56
csf1	Colony-stimulating factor 1	Cytokine for osteoclast activation	2.60†	1.85†	2.49†
c-fms	Receptor for Csf1	Osteoclast activation	2.02†	2.01†	−1.20
Itgb3	β3 integrin	Osteoclast attachment	1.01	2.22†	2.30†
Ibsp	Integrin binding sialoprotein	Osteoclast attachment, cell migration	2.09†	−1.16	−1.01
Adam8	Disintegrin and metalloproteinase domain 8	Osteoclast activation	2.43†	2.00†	2.03†
Trem2	Triggering receptor expressed on myeloid cells 2	DAP12-associated receptor, regulates osteoclast differentiation and function	2.15†	2.11†	2.25†
Oscar	Osteoclast associated receptor	Osteoclast activation	2.15†	2.49†	2.19†
PLCγ	Phospholipase Cγ	Signal transduction	2.06†	2.06†	−1.30
c-Fos	c-Fos–induced growth factor	Signal transduction	2.04†	2.10†	−1.25
Nfatc1	Nuclear factor of activated T cells	Transcriptional factor for T cell activation	2.02†	2.01†	−1.20
c-Src	c-Src tyrosine kinase	Cytoskeleton organization	2.01†	1.02	2.02†
Syk	Spleen tyrosine kinase	Cytoskeleton organization	2.02†	1.03	2.17†
Vav3	Vav 3 oncogene	Cytoskeleton organization	2.12†	2.28†	2.39†
ATPase	ATPase, H+ transporting	Acidified microenvironment	2.20†	2.13†	2.08†
Mmp9	Matrix metalloproteinase 9	Matrix degradation	2.12†	2.03†	2.01†
Ctsk	Cathepsin K	Matrix degradation	2.01†	2.07†	2.11†
Prss22	Protease, serine, 22	Matrix degradation	1.03	2.35†	2.38†

*Values are the fold change versus day 0 (placebo group, set at 1).

†$P < 0.05$ versus day 0.

Table 2

Time-dependent effects of glucocorticoid excess on the expression of selected adipocyte-specific genes*

Gene symbol	Gene name	Gene function	Day 7	Day 28	Day 56
c/EBPα	CCAAT/enhancer binding protein α	Adipocyte differentiation	2.06†	−1.05	−1.00
c/EBPβ	CCAAT/enhancer binding protein β	Adipocyte differentiation	2.08†	1.00	1.06
PPARγ	Peroxisome proliferator–activated receptor γ	Adipocyte differentiation	2.04†	1.01	−1.07
PPARσ	Peroxisome proliferator–activated receptor σ	Adipocyte differentiation	2.08†	−1.04	1.00
AdipoQ	Adiponectin, C1Q and collagen domain containing	Differentiated adipocytes	2.03†	2.16†	2.12†

*Values are the fold change versus day 0 (placebo group, set at 1).

†$P < 0.05$ versus placebo.

Arthritis Rheum. Author manuscript; available in PMC 2014 January 15.